Resonant Electron Heating and Molecular Phonon Cooling in Single C_{60} Junctions

G. Schulze,[1] K. J. Franke,[1] A. Gagliardi,[2] G. Romano,[3] C. S. Lin,[2] A. L. Rosa,[2] T. A. Niehaus,[2] Th. Frauenheim,[2] A. Di Carlo,[3] A. Pecchia,[3] and J. I. Pascual[1]

[1]*Institut für Experimentalphysik, Freie Universität Berlin, Arnimallee 14, 14195 Berlin, Germany*
[2]*Bremen Center for Computational Materials Science, University of Bremen, D-28359, Germany*
[3]*Università di Roma "Tor Vergata," 00133 Roma, Italy*

(Received 14 December 2007; published 2 April 2008)

We study heating and heat dissipation of a single C_{60} molecule in the junction of a scanning tunneling microscope by measuring the electron current required to thermally decompose the fullerene cage. The power for decomposition varies with electron energy and reflects the molecular resonance structure. When the scanning tunneling microscope tip contacts the fullerene the molecule can sustain much larger currents. Transport simulations explain these effects by molecular heating due to resonant electron-phonon coupling and molecular cooling by vibrational decay into the tip upon contact formation.

DOI: 10.1103/PhysRevLett.100.136801 PACS numbers: 73.63.−b, 68.37.Ef, 73.61.Wp

The paradigm of molecular electronics is the use of a single molecule as an electronic device [1]. This concept is sustained on the basis that a single molecule (or a molecular thin film) should withstand the flow of electron current densities as large as 10^{10} A/m^2 without degrading. A fraction of these electrons heat the molecular junction through inelastic scattering [2]. The temperature at the junction is a consequence of an equilibrium between heating and heat dissipation out of the junction. The former is dominated by the coupling of electronic molecular states with molecular vibrons [2–4]. The latter depends on the strength of the vibrational coupling between the "hot" molecular vibrons and the bath degrees of freedom of the "cold" electrodes.

Theoretical studies predicted that current-induced heating in molecular junctions can be large enough to affect the reliability of molecular devices [2]. However, experimental access to this information is very limited. Recent studies of the thermally activated force during molecular detachment from a lead [5,6] and of structural fluctuation during attachment to it [7] reveal that the temperature of a molecular junction can reach several hundred degrees under normal working conditions, thus evidencing that present devices work on the limit of practical operability [8]. Heat dissipation away from the junction becomes an important issue.

In this Letter, we characterize the mechanisms of heating and heat dissipation induced by the flow of current across a single molecule. Our approach is based on detecting the limiting electron current inducing molecular decomposition at varying applied source-drain bias (i.e., the maximum power one molecule can sustain). We use a low temperature scanning tunneling microscope (STM) to control the flow of electrons through a single C_{60} molecule at an increasing rate until the molecule decomposes. By comparing the power applied for decomposition (P_{dec}) in the tunneling regime and in contact with the STM tip we find that it depends significantly on two factors: (i) P_{dec} decreases when molecular resonances participate in the transport, evidencing that they enhance the heating; (ii) P_{dec} increases as the molecule is contacted to the source and drain electrodes, revealing the heat dissipation by phonon coupling to the leads. A good contact between the single-molecule device and the leads is hence an important requirement for its operation with large current densities.

Our experiments are carried out in a custom-made ultrahigh vacuum STM at a temperature of 5 K. We choose a Cu(110) single crystal surface because here C_{60} adsorbs in a well-defined configuration, between 4 of the topmost Cu atoms [9]. By annealing a submonolayer film of C_{60} to 470 K we produce ordered fullerene islands with a pseudohexagonal structure [Fig. 1(a)], in which C_{60} adsorbs keeping a pentagon-hexagon C-C bond pointing upwards. Scanning tunneling spectroscopy [Fig. 1(b)] shows a clear spectroscopic fingerprint characterized by a strong resonance at 1.5 eV above the Fermi level, and associated to the LUMO + 1 resonance (LUMO: lowest unoccupied molecular orbital). The LUMO appears as a weaker broader peak around 0.2 eV and is partially occupied [10]. A spectrum like the one in Fig. 1(b) is thus taken here as a litmus test for the integrity of the C_{60} molecule.

In our experiment, we approach the STM tip [11] a distance Z_{appr} towards a single C_{60} at constant sample bias (V_s) and record the current flowing through the molecule [$I(Z_{\mathrm{appr}})$]. The tunnel regime [identified as the exponential regime in the $I(Z_{\mathrm{appr}})$ plots] extends until the junction conductivity reaches $\sim 0.03 G_0$ ($G_0 = 77.5\ \mu$S). Beyond this point, a tip-C_{60} contact starts to be formed and the $I(Z_{\mathrm{appr}})$ plots deviate smoothly from the exponential behavior [7,12]. C_{60} is very stable under the proximity of the STM tip. If a small positive sample bias ($V_s < 0.6$ V) is used, C_{60} withstands tip contact and indentations of several Ångstroms, holding currents close to 100 μA [Fig. 1(c)].

When V_s is increased above 0.6 V, C_{60} degrades during the tip approach, as we could identify from three facts

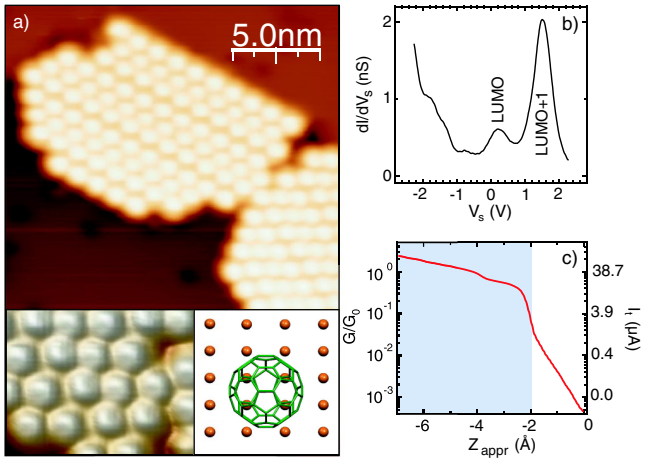

FIG. 1 (color online). (a) STM image of a 0.2 monolayer film of C_{60} on Cu(110) ($I_t = 1.1$ nA, $V_s = 1.75$ V). The intramolecular structure (left inset; $I_t = 1.0$ nA, $V_s = 2.25$ V [29]) reveals an intrinsic asymmetry consistent with the adsorption orientation from density functional theory simulations (right inset). (b) Differential conductivity spectrum of C_{60} ($R_{\text{junct}} = 2.2\ \text{G}\Omega$, lock-in amplifier: $V_{\text{ac}} = 20$ mV rms). (c) Conductance and current vs Z_{appr} plot on top of a C_{60} molecule ($V_s = 0.5$ V). The shaded area indicates the contact regime.

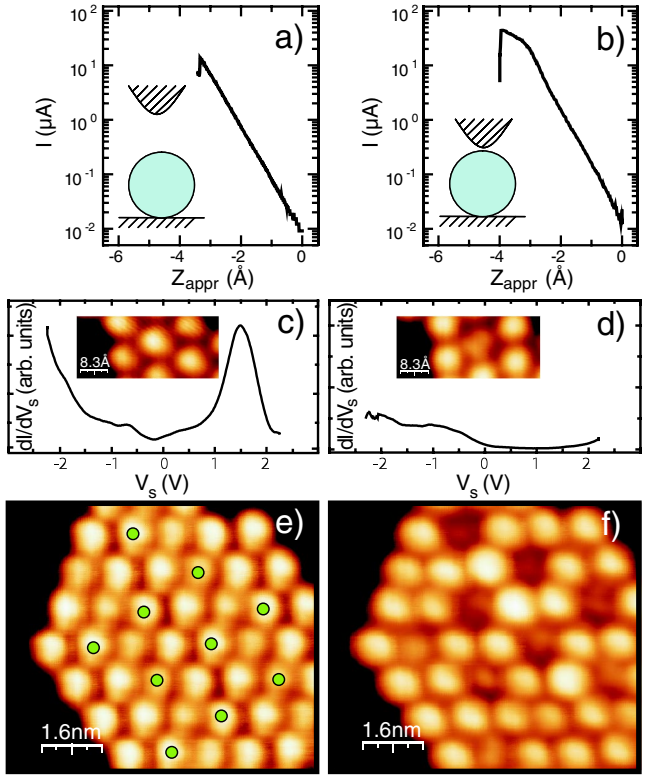

FIG. 2 (color online). $I(Z_{\text{appr}})$ plots showing molecular decomposition in (a) tunnel ($V_s = 2.0$ V) and (b) contact regime ($V_s = 1.0$ V). (c) Scanning tunneling spectroscopy spectrum of a molecule before and (d) after an $I(Z_{\text{appr}})$ plot like in panel (a). The resonance structure disappears, thus indicating destruction of the fullerene cage. (e) C_{60} island before and (f) after performing $I(Z_{\text{appr}})$ events on the molecules marked in (e). After this, all the marked molecules show a lower height and a dI/dV spectrum similar to panel (d) ($I_t = 1.0$ nA, $V_s = 2.25$ V).

(Fig. 2): (i) a sharp discontinuity in the $I(Z_{\text{appr}})$ plots indicates an irreversible change in the molecule; (ii) the height of the degraded molecule is typically more than 1 Å lower than its neighbors; (iii) the dI/dV_s spectrum reveals that the characteristic resonance structure vanishes. The precise way in which C_{60} is degraded cannot be determined in our measurements. The disappearance of molecular resonances in the spectra hints that the most probable result is a rupture of the icosahedral carbon cavity. The decomposition is observed solely on the molecule selected for the indentation. Thus, we can discard an electron-induced polymerization with neighboring molecules [13].

A current drop as in Figs. 2(a) and 2(b) provides the position Z_{dec} and current I_{dec} at which molecular decomposition occurs. Both Z_{dec} and I_{dec} depend strongly on the bias value V_s. In Fig. 3(a) we plot the statistical average of I_{dec} as a function of V_s between 0.6 to 3.0 V. For $V_s = 3.0$ V an electron current $I_{\text{dec}} = 7\ \mu$A suffices to degrade the C_{60}. This occurs when the tip is still more than 1 Å away from the contact position, i.e., in the tunnel regime. As V_s is reduced I_{dec} increases gradually (with a small plateau around 1.5 and 2.5 eV), and accordingly decomposition occurs with the tip closer to the fullerene, but still in the tunnel regime [i.e., with $I(Z_{\text{appr}})$ curves as in Fig. 2(a)]. For V_s below $\sim$1.2 V a more pronounced increase of I_{dec} is observed. In this range the onset of tip-C_{60} contact is already detected in the $I(Z_{\text{appr}})$ plots [as in Fig. 2(b)]. Electron currents as high as 70 μA can flow through the molecular junction for the lowest bias achieving degradation ($V_s \sim 0.6$ V). In this regime the STM tip indents more than 2 Å beyond the contact position. However, we can rule out a mechanical process of rupture because below the threshold bias of 0.6 V C_{60} remains unaffected upon tip indentations of more than 4 Å [see Fig. 1(c)]. Instead, we note that C_{60} undergoes a thermal decomposition on surfaces at temperatures around 1000 K [14–17]. Thus, we consider that the decomposition of C_{60} is a *current-driven* thermal process, where the critical current depends crucially on the applied voltage.

The two different regimes of molecular decomposition in tunnel and in contact as suggested in Fig. 3(a) become more evident when we plot the power P_{dec} ($P_{\text{dec}} = I_{\text{dec}} \times V_s$) applied to the C_{60} junction for its degradation [Fig. 3(b)]. In the tunnel regime, i.e., above $V_s \sim 1.2$ V, P_{dec} amounts to $\sim$20 μW and shows small oscillations at the LUMO + 1 and LUMO + 2 position. For lower bias P_{dec} increases sharply up to more than 50 μW, reflecting that here the junction can sustain larger current densities. In this regime decomposition is attained when the tip is in contact with the molecule. Hence, the very sharp change in P_{dec} as compared to the oscillations in P_{dec} around higher

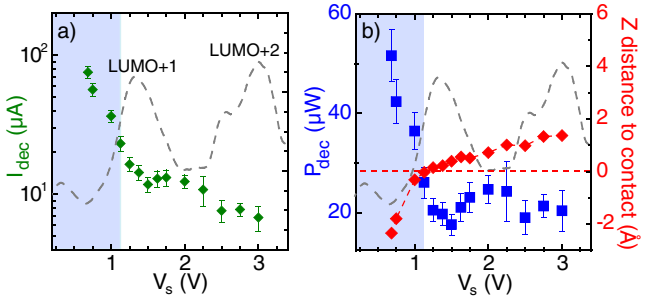

FIG. 3 (color online). (a) Statistical average of I_{dec} vs V_s with two sigma error bars. All the events considered (180) correspond to degradation as in Fig. 2, and were done on fullerenes surrounded by unperturbed C_{60} molecules. (b) Bias dependence of P_{dec} (squares) and distance to contact Z (diamonds). For events in the tunnel regime, Z_{dec} is obtained by linear extrapolation. Shaded areas indicate decomposition in the contact regime. Dashed lines represent normalized dI/dV_s plots.

molecular resonances suggests that the contact plays an important role for the decomposition process.

The origin of molecular dissociation in the two different transport regimes can be rationalized from a conceptual definition of molecular temperature. The electron tunneling rates used to decompose the C_{60} molecule are larger than typical phonon decay rates for adsorbate systems. Hence, we consider a current-induced heating, in which C_{60} vibrations are excited in a nonequilibrium distribution [18,19]. For a certain set of current and bias values, the total vibrational energy U_m stored in the molecule (and hence its temperature T_m) depends on the balance between the *heat generated* by the inelastic scattering of electrons with molecular modes, and *heat dissipation* into the cold leads ($T = 5$ K) [2,4,20]. Following this picture, a larger degradation power P_{dec} is due to either a less effective heat generation or to a more effective dissipation of heat into the leads.

To analyze and corroborate the influence of the resonances and the tip-molecule contact we have performed model transport calculations based on the nonequilibrium Green's function formalism [21,22]. The C_{60} molecule is relaxed on a slab of 8 layers of copper in a 4×5 unit cell using density functional theory calculations [23]. The resulting structure is in good agreement with experiments [9]. The LUMO, LUMO + 1, and LUMO + 2 states are located at 0.7, 1.5, and 3.0 V above the Fermi level, respectively. The tip is represented by a Cu atom adsorbed on a jellium surface.

Inelastic electron scattering in C_{60} is calculated using the self-consistent Born approximation [24]. The nonequilibrium phonon population, N_q (where the q index runs over all 174 normal modes of vibration of C_{60}), is deduced from a rate equation including the phonon absorption (A_q) and emission probabilities (E_q) in the device calculated as in Ref. [20]. A "model" molecular temperature T_m can be associated to the internal energy, $U_m = \sum_q h\nu_q N_q$, by assuming a Bose-Einstein phonon population that produces the same internal energy as the nonequilibrium population N_q [25].

Figure 4(a) shows the effect of increasing the applied bias on T_m. For the experimental values of tip-molecule distance, the applied bias leads to a heating of the molecule above 1000 K. Such high temperatures are reached with only a small fraction of electrons being inelastically scattered by molecular vibrons ($\sim 10^{-3}$). The heating becomes more effective when the LUMO resonance enters in conduction due to resonant electron-phonon emission [4]. The temperature increase is largest when all the C_{60} vibrational band (200 meV width) can be excited. A similar rise in T_m appears at bias values when higher order resonances enter into conduction. Contrary to this, phonon assisted tunneling contributes to cooling the C_{60} molecule right below the resonances, causing in total a modulated rise in T_m.

To simulate the experimental curves of Fig. 3, we set a critical temperature for decomposition, T_{dec}, and obtain from Fig. 4(a) the corresponding set of values V_{dec} and Z_{dec}. From the I–V characteristics we then extract the corresponding I_{dec}. For $T_{dec} \sim 1650$ K the applied power is similar to the experimental values [26]. For bias values larger than 1.2 V the decomposition takes place in the tunnel regime and a steplike behavior is obtained for I_{dec}.

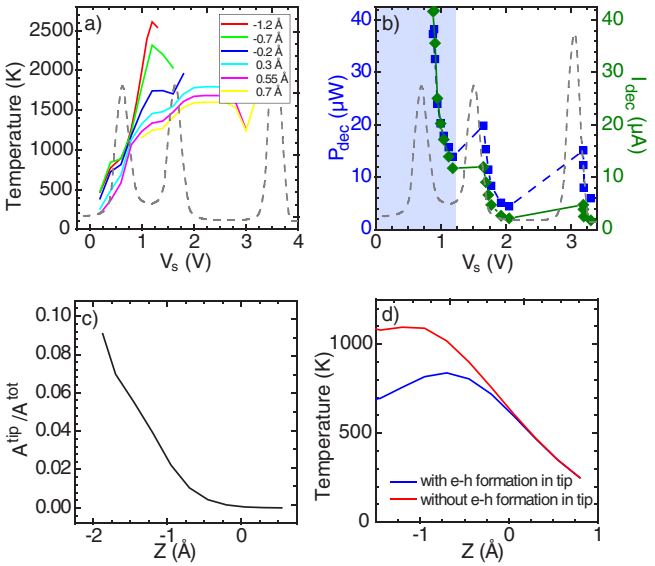

FIG. 4 (color online). Results of theoretical simulations: (a) T_m vs V_s for the indicated distances to contact. The oscillations of T_m are associated to the molecular resonances (dashed line). (b) The values I_{dec} (diamonds, continuous line) and P_{dec} (squares, dark broken line) are marked for a threshold temperature of 1650 K of the C_{60} molecule. The shaded area marks the contact regime. (c) Ratio of the phonon absorption rate (A^{tip}) to the total absorption rate in the junction (A^{tot}) vs tip-molecule distance (tip-molecule contact is defined as 0 Å) at 0.4 V. (d) T_m at 0.4 V vs tip-molecule distance with (lower line) and without (upper line) electron-hole pair formation in the tip.

Where I_{dec} remains constant P_{dec} increases, thus producing the oscillations shown in Fig. 4(b). These reflect the resonant phonon cooling and heating below and above a resonance, respectively. Such oscillations resemble the experimental oscillations of P_{dec} at the LUMO + 1 and LUMO + 2, hence confirming a resonance mediated mechanism of molecular heating in tunneling.

This, however, does not explain the very large increase in P_{dec} for sample bias below 1.2 V. Here, as in the experiment, molecular decomposition is achieved once the tip is in contact with C_{60}. The tip-molecule contact enhances the dissipation of vibrations from the hot molecule into the cold tip. There are two possible mechanisms of mode quenching: vibrational decay into substrate phonons and into electron-hole (e-h) pair excitations. Our calculations suggest that the former plays a small role in the cooling effect, since the phonon bands at the leads are much narrower than the C_{60} vibrational spectrum. On metal surfaces, instead, the main mechanism is the e-h excitation in the leads [27]. From our calculations we can estimate the contribution of e-h pair creation in the tip by extracting the corresponding phonon absorption rate (A_q^{tip}) [28]. Molecular mode quenching becomes important in the proximity of contact formation and further indentation in the molecule as revealed by the monotonic increase of A_q^{tip} [Fig. 4(c)]. The effect on T_m can be determined by setting A_q^{tip} to zero and calculating again the effective temperature. Figure 4(d) evidences that the temperature thus determined increases much faster when approaching the tip towards the molecule than in the case where e-h excitation in the tip is allowed. This strongly supports that the sharp increases in I_{dec} and P_{dec} result from vibrational cooling upon contact formation. At low bias, the LUMO resonance starts to be removed from the conduction window and, as shown in Fig. 4(a), the molecular temperature decreases drastically. This explains that the thermal decomposition cannot be achieved in the experiment below 0.6 eV.

In summary, our results reveal that resonant tunneling through molecular states in a single-molecule device can generate sufficient heat to thermally decompose the molecular junction. For the case of a C_{60} molecule on a Cu(110) surface, a power of 20 μW is sufficient. To increase the current density a molecular junction can sustain, it would be useful to remove molecular resonances from the transport window. However, in most cases the molecular device properties rely crucially on molecular resonances, and hence cannot be engineered without losing the functionality. Good contact of the molecule with the leads then opens the possibility for the single-molecule device to withstand larger current densities.

This research was supported by the DFG through Grants No. SPP 1243 and No. Sfb 658.

[1] A. Aviram and M. Ratner, Chem. Phys. Lett. **29**, 277 (1974).
[2] M. Galperin, M. A. Ratner, and A. Nitzan, J. Phys. Condens. Matter **19**, 103201 (2007).
[3] M. Galperin, A. Nitzan, and M. A. Ratner, Phys. Rev. B **75**, 155312 (2007).
[4] A. Pecchia, G. Romano, and A. Di Carlo, Phys. Rev. B **75**, 035401 (2007).
[5] Z. Huang *et al.*, Nano Lett. **6**, 1240 (2006).
[6] Z. Huang *et al.*, Nature Nanotechnology **2**, 698 (2007).
[7] N. Neel *et al.*, Phys. Rev. Lett. **98**, 065502 (2007).
[8] J. M. Tour, Acc. Chem. Res. **33**, 791 (2000).
[9] R. Fasel *et al.*, Phys. Rev. B **60**, 4517 (1999).
[10] These values remain down to tip-molecule contact.
[11] Indenting the tip into clean surface areas ensures the tip apex to consist of Cu atoms.
[12] C. Joachim *et al.*, Phys. Rev. Lett. **74**, 2102 (1995).
[13] Y. B. Zhao *et al.*, Appl. Phys. Lett. **64**, 577 (1994).
[14] C. Cepek, A. Goldoni, and S. Modesti, Phys. Rev. B **53**, 7466 (1996).
[15] J. I. Pascual, J. Gomez-Herrero, and A. M. Baro, Surf. Sci. **397**, L267 (1998).
[16] N. Swami, H. He, and B. E. Koel, Phys. Rev. B **59**, 8283 (1999).
[17] V. Saltas and C. A. Papageorgopoulos, Surf. Sci. **488**, 23 (2001).
[18] S. Gao, Phys. Rev. B **55**, 1876 (1997).
[19] G. P. Salam, M. Persson, and R. E. Palmer, Phys. Rev. B **49**, 10 655 (1994).
[20] G. Romano, A. Pecchia, and A. Di Carlo, J. Phys. Condens. Matter **19**, 215207 (2007).
[21] A. Pecchia and A. Di Carlo, Rep. Prog. Phys. **67**, 1497 (2004).
[22] A. Gagliardi *et al.*, Phys. Rev. B **75**, 174306 (2007).
[23] M. Elstner *et al.*, J. Chem. Phys. **114**, 5149 (2001).
[24] M. Galperin, M. Ratner, and A. Nitzan, Nano Lett. **4**, 1605 (2004).
[25] A better approach employs a fictitious external phonon bath to "measure" T_m [2]. Qualitatively, both methods are similar.
[26] No qualitative difference is seen in the results if T_{dec} is increased by several hundred degrees or by using U_m as a critical parameter for molecular decomposition.
[27] S. Gao, M. Persson, and B. I. Lundqvist, Solid State Commun. **84**, 271 (1992).
[28] The excitation of an e-h pair in the tip can be seen as a process in which an electron from the tip absorbs a phonon and is reflected back into the tip: $A_q^{tip} = 2/h \int_{-\infty}^{\infty} \mathrm{Tr}[R_t \times \alpha_q \times R_t \times \alpha_q]\{f_t(E - \hbar w_q)[1 - f_t(E)]\}dE$, ($\alpha_q$: electron-phonon coupling matrix, R_t: projected density of states on C_{60} + tip states, f_t: tip Fermi function).
[29] I. Horcas *et al.*, Rev. Sci. Instrum. **78**, 013705 (2007).